Characterization of Muscarinic Acetylcholine Receptors in the Avian Salt Gland

SETH R. HOOTMAN and STEPHEN A. ERNST
Department of Anatomy and Cell Biology, University of Michigan, Medical Sciences II, Ann Arbor, Michigan 48109

ABSTRACT Electrolyte and fluid secretion by the avian salt gland is regulated by activation of muscarinic acetylcholine receptors (R). In this study, these receptors were characterized and quantitated in homogenates of salt gland from domestic ducks adapted to conditions of low (freshwater, FW) and high (saltwater, SW) salt stress using the cholinergic antagonist [^{3}H]-quinuclidinyl benzilate (QNB). Specific binding of the antagonist to receptors in both FW- and SW-adapted glands reveals a single population of high affinity binding sites (K_{dFW} = 40.1 ± 3.0 pM; K_{dSW} = 35.1 ± 2.1 pM). Binding is saturable; RL_{maxFW} = 1.73 ± 0.10 fmol/μg DNA; RL_{maxSW} = 4.16 ± 0.31 fmol/μg DNA (where L is [^{3}H]QNB and RL the high affinity complex). Calculated average cellular receptor populations of 5,800 sites/cell in FW-adapted glands and 14,100 sites/cell in SW-adapted glands demonstrate that upward regulation of acetylcholine receptors in the secretory epithelium follows chronic salt stress. The receptor exhibits typical pharmacological specificities for muscarinic cholinergic antagonists (QNB, atropine, scopolamine) and agonists (oxotremorine, methacholine, carbachol). In addition, the loop diuretic furosemide, which interferes with ion transport processes in the salt gland, competitively inhibits [^{3}H]QNB binding. Preliminary studies of furosemide effects on [^{3}H]QNB binding to rat exorbital lacrimal gland membranes showed a similar inhibition, although the diuretic had no effect on antagonist binding to rat brain or atrial receptors.

The avian salt gland provides a rather unique model for the study of exocrine secretion of electrolytes since, unlike most other vertebrate exocrine organs, it produces an effluent that contains only trace amounts of protein or other macromolecular species. The principal solutes present in the hypertonic secreted fluid are Na^+ and Cl^-, the concentrations of which may range from 500 to 900 mEq/l (25). The onset of secretion by the quiescent salt gland appears to be mediated primarily via activation of muscarinic acetylcholine receptors. This view is supported by the following evidence. (*a*) Intravenous injection of anesthetized herring gulls with acetylcholine or methacholine stimulates salt gland secretion, while secretion in response to either a parenteral salt load or to a direct stimulation of the secretory nerve is blocked by injection of atropine (11). (*b*) The secretory nerve is rich in cholinergic fibers which ramify throughout the glandular parenchyma (1). (*c*) Exposure of salt gland tissue slices or dispersed salt gland cells in vitro to cholinergic agonists elicits a number of secretion-related responses. These include increases in ouabain-sensitive oxygen consumption (2, 16, 39), stimulation of Na^+ efflux (42), potentiation of Na^+ pump activity (17), and an increase in cellular cyclic GMP levels (39).

In addition to regulating acute secretory events in the avian salt gland, cholinergic innervation also appears to play a central role in maintenance of the gland's differentiated state. When domestic ducks or geese adapted to freshwater are allowed only saltwater to drink, a procedure that stimulates almost continual salt secretion, the salt glands rapidly hypertrophy. This growth is accomplished through a combination of proliferation of cells in the glandular parenchyma and hypertrophy of individual secretory cells (8), the end result being a greatly amplified glandular secretory capacity. Functional hypertrophy in response to chronic salt stress can be blocked, however, by ablation of the secretory nerve (14, 27). These results suggest that the increased frequency of nervous stimulation that accompanies chronic salt stress plays both initiating and sustaining roles during the respose to functional demand in the avian salt gland. Of interest in this regard is the question of whether or not muscarinic receptor populations are present in the gland and, if so, whether they are increased during the period of basolateral plasma membrane hypertrophy that follows chronic salt loading. This is a particularly intriguing question, since

THE JOURNAL OF CELL BIOLOGY · VOLUME 91 DECEMBER 1981 781-789

recent studies on cultured neuroblastoma cells (37) and on intact rat brain (35) have demonstrated decreases in the number of muscarinic acetylcholine receptors per cell following chronic receptor activation.

Here we report the results of investigations designed to quantitate and characterize acetylcholine receptors in salt glands of domestic ducks adapted to conditions of both high and low salt stress, using the radiolabeled muscarinic antagonist [^{3}H]quinuclidinyl benzilate ([^{3}H]QNB). These studies demonstrate the presence of a population of muscarinic receptors in salt gland cell membranes and define their pharmacological specificities. Our findings also show for the first time that proliferation of muscarinic acetylcholine receptors can accompany the response to functional demand in an ion secreting epithelium where these receptors play a regulatory role.

MATERIALS AND METHODS

Animals

2- to 3-d-old Pekin ducks (*Anas platyrhynchos*) were received from Ridgeway Hatcheries (LaRue, Ohio) and maintained for 1 wk on tapwater and a commercial poultry feed. After 1 wk, the ducklings were separated into two groups. One group continued to receive freshwater while the other received drinking water containing 1% NaCl. Ducks were maintained on these two regimens for several months, but were not used for experiments until at least 1 month of age. Adult Sprague-Dawley rats of both sexes were obtained from Blue Spruce Farms (Altamont, N.Y.) and maintained on lab chow and tapwater.

Reagents

The following reagents were obtained from Sigma Chemical Co. (St. Louis, Mo.): acetyl-β-methylcholine chloride (methacholine), atropine sulfate, bovine serum albumin (BSA), calf thymus DNA, Carbamylcholine chloride (carbachol), ouabain, oxotremorine, and scopolamine hydrobromide. Furosemide and bumetanide were generous gifts from Hoechst-Roussel Pharmaceuticals, Inc. (Somerville, N.J.). Unlabeled DL-quinuclidinyl benzilate was obtained from Hoffman-La Roche, Inc. (Nutley, N.J.). [^{3}H]L-quinuclidinyl benzilate (40.2 Ci/mmol) was purchased from New England Nuclear Corp. (Boston, Mass.). Reagents for electron microscope preparation of salt gland tissue samples were obtained from Electron Microscopy Sciences (Fort Washington, Pa.). All other chemicals used were of reagent grade quality.

Tissue Preparation

Ducks were killed and the paired salt glands were excised, trimmed of adherent connective tissue, and weighed. The glands were then minced and homogenized in ice-cold 0.05 M sodium phosphate buffer (pH 7.4) to a concentration of 10 mg of wet tissue weight/ml. Homogenates were filtered once through 50-μm nylon mesh and held on ice. Aliquots of these homogenates were frozen for later protein and DNA analysis. Rats were killed and the brain, heart atria, and exorbital lacrimal glands were excised and weighed. These organs were then separately homogenized as above and held on ice.

[^{3}H]QNB Binding Assay

The binding assay used in these studies was a modification of that developed by Yamamura and Snyder (43). Incubations were carried out in 5.0 ml total volumes of 0.05 M sodium phosphate buffer (pH 7.4) containing various amounts of homogenate protein, [^{3}H]QNB, and other drugs. Duplicate tubes containing 1.0 μM atropine sulfate were included in each assay and specific [^{3}H]QNB binding was determined as the difference in binding in the absence and presence of atropine. Incubations were begun by the addition of 0.5-ml aliquots of fresh homogenate (50–300 μg of protein) to tubes containing 4.5 ml of incubation medium and were carried out at 37°C with continuous agitation for various periods. Experimental points were determined in duplicate in most instances. Binding assays were terminated by pouring the incubated suspensions onto GF/B glass fiber filters (Whatman, Inc., Chemical Separation Div., Clifton, N.J.) mounted in a Millipore vacuum filtering apparatus. Filters were then rinsed four times with 5.0-ml aliquots of cold incubation buffer. Rinsed filters were placed in scintillation vials and extracted for several hours with frequent vortexing in a 1:10 mixture of Protosol and Omnifluor (NEN) and counted in a Beckman LS 9000 liquid scintillation spectrometer (Beckman Instruments, Spinco Div., Palto Alto, Calif.). In each experiment, duplicate filters were also analyzed for protein content following extraction for 16–20 h in 1.0 ml of 0.5 N NaOH/5% SDS.

Analysis of Data

In analysis of data from [^{3}H]QNB saturation binding and kinetic experiments, we made the assumption that the antagonist-receptor interaction under our assay conditions could be defined by the simple bimolecular reaction mechanism represented by the equation:

$$L + R \underset{k_{-1}}{\overset{k_{+1}}{\rightleftarrows}} RL$$

where L is [^{3}H]QNB, R represents the acetylcholine receptor, and RL is the high affinity complex formed. k_{+1} and k_{-1} are the rate constants for formation and dissociation of the receptor-ligand complex. The derivation of formulas for determining these constants, the equilibrium dissociation constant (K_d), and other parameters of binding is covered in detail in recent papers by Fields et al. (12) and Hartzell (15) and is therefore not presented here.

Protein and DNA Assays

DNA in homogenates was determined by the Burton diphenylamine procedure, as modified by Croft and Lubran (6), using calf thymus DNA as a standard. Protein in homogenates and on filters was determined by a modification of the Lowry procedure (26), using crystalline BSA as a standard.

Electron Microscopy

Minced pieces of salt gland from freshwater(FW)- and saltwater(SW)-adapted ducks were fixed by immersion for 2 h at room temperature in 1% formaldehyde–1.5% glutaraldehyde buffered to pH 7.4 with 0.1 M sodium cacodylate and further processed for electron microscopy as described previously (16).

RESULTS

Adaptive Response to Salt Stress

The fine structure of the duck salt gland and the adaptive response of the gland to chronic salt stress have been described previously (8, 9) and therefore will not be discussed in detail here. The data in Fig. 1 and Table I are included for orientation purposes and to define the adaptive response under the present experimental conditions. The parenchyma of the salt gland consists of closely packed tubules of simple cuboidal epithelium (Fig. 1). Individual secretory cells are characterized by numerous mitochondria and an elaborately folded basolateral plasma membrane. The primary morphological difference between secretory cells in animals adapted to FW or SW is a great increase in the degree of plasma membrane elaboration in the latter (Fig. 1 *inset*). This salt-induced hypertrophic change in the cytoarchitecture of the secretory cell is mirrored when one biochemically examines selected glandular constituents (Table I). The salt glands of ducks adapted to SW are roughly four times as large as their counterparts in ducks maintained on FW. This vast hypertrophy results in part from cellular hyperplasia ($DNA_{SW}/DNA_{FW} = 2.67$). In addition, the amplification of plasma membrane and mitochondria seen in micrographs of individual salt-stressed secretory cells is reflected in an increased protein-to-DNA ratio (22.8 mg protein/mg DNA in SW-adapted glands vs. 13.0 mg protein/mg DNA in FW glands).

Nerve endings are abundant in both FW- and SW-adapted salt glands. In both, they are closely associated with the basal surfaces of secretory cells (Fig. 2). These termini commonly contain abundant 30- to 40-nm electron lucent vesicles and less numerous larger vesicles (80 to 120-nm) that display electron-dense central cores.

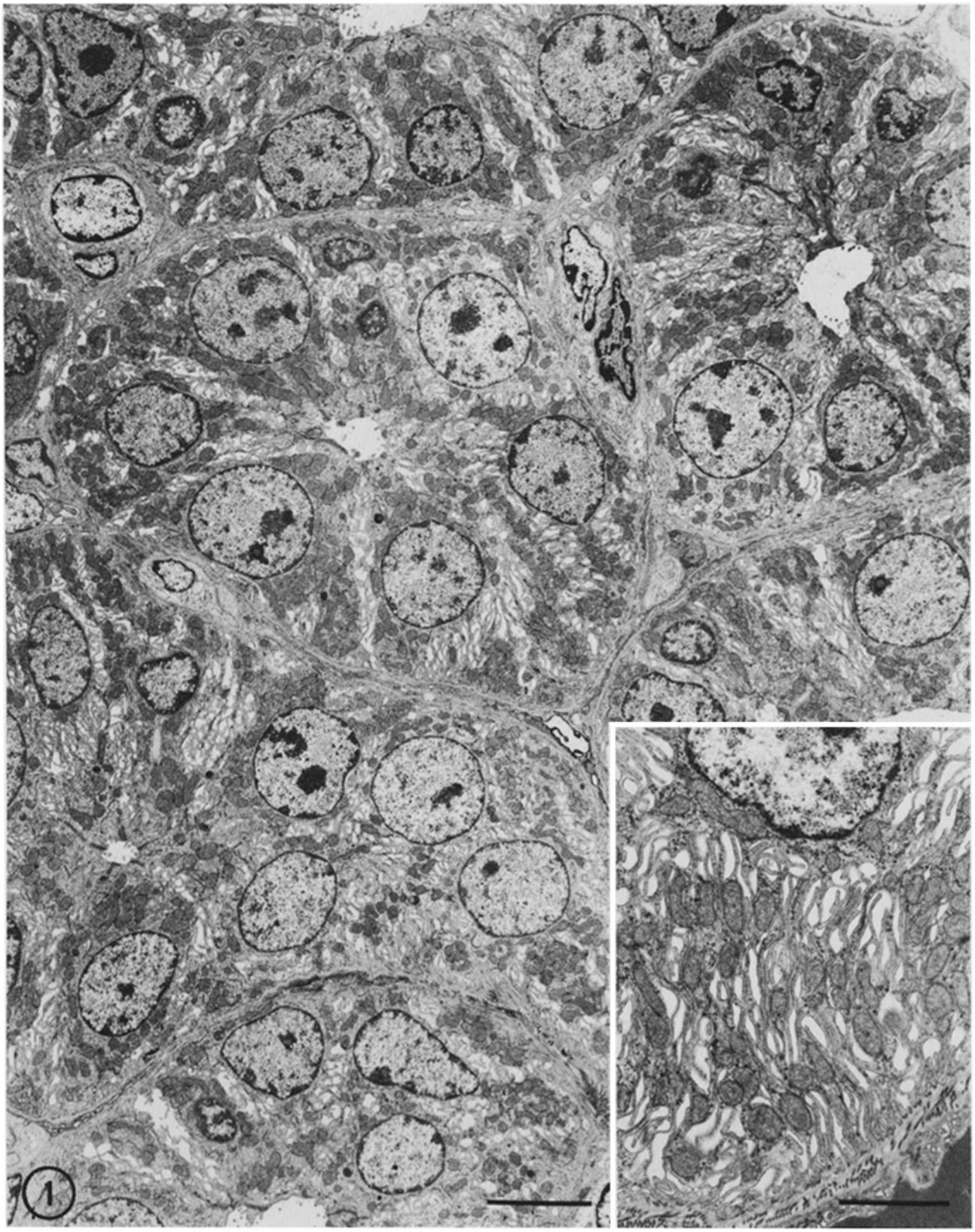

FIGURE 1 Electron micrograph of the secretory parenchyma from a salt gland of a duck adapted to FW. The epithelium consists of a homogenous mass of tightly packed tubules of simple cuboidal epithelium. The lateral cell surfaces of individual secretory cells are extensively folded and are closely associated with many mitochondria. *Inset:* electron micrograph of the basal portion of a secretory epithelial cell from a salt gland of a duck adapted to 1% NaCl for several weeks. Folding of the basolateral plasma membrane is now extreme. Mitochondria are more numerous than in cells of nonstressed glands and are encapsulated within basolateral membrane folds in many cases. Bar, 5 μm. *Inset* bar, 2 μm. × 3,700. *Inset,* × 9,400.

Characteristics of [^{3}H]QNB Binding

In our initial experiments, homogenates of salt gland from each of five FW- and SW-adapted ducks of equal age were prepared and diluted to three concentrations; 2, 4, and 6 mg wet weight/ml. These dilutions resulted in final protein concentrations in the incubations ranging from 15 to 60 μg/ml. Equilibrium binding at each of these concentrations was then determined at concentrations of [^{3}H]QNB ranging from 25 to 600 pM. A typical saturation binding isotherm is shown in Fig. 3 *a*. Binding consisted of both specific and nonspecific components. The former was saturable and approximated a rectangular hyperbola, indicating a single population of receptors of high affinity. Scatchard analysis of such curves invariably generated a single straight line (Fig. 3 *b*). The average correlation coefficients (*r*) for fifteen determinations on salt gland homogenates from each salinity regimen were 0.974 for FW-adapted and 0.945 for SW-adapted glands. In contrast, the nonspecific component of binding, determined in the presence of 1 μM atropine sulfate, was linearly dependent on [^{3}H]QNB concentration up to 600 pM and showed no tendency toward saturation (Fig. 3 *a*). From each specific binding curve, Scatchard analysis was used to determine both a saturation binding value (RL_{max}) and an equilibrium dissociation constant (K_d) for the receptor-ligand interaction. No specific differences ($P > 0.05$) were noted in RL_{max} at the three concentrations of each homogenate assayed, indicating a linear dependence of [^{3}H]-QNB binding on tissue concentration up to at least 60 μg protein/ml. Dissociation constants for binding to both FW-adapted and SW-adapted salt glands were also not influenced significantly by changes in tissue concentration over this range. Average values for these two binding parameters are shown in Table II. The K_d for [^{3}H]QNB binding in FW-adapted salt glands was 40.1 ± 3.0 pM and that in SW-adapted glands was 35.1 ± 2.1 pM. These values are not significantly different from one another ($P > 0.05$), indicating that the affinity of the muscarinic receptor for the antagonist is not altered during

TABLE I

Comparison of Gland Weights, Protein, and DNA in Salt Glands of FW- and SW-adapted Ducks

	Wet weight	Protein	DNA
	g	*mg*	*mg*
FW-adapted	0.24 ± 0.02	21.2 ± 2.0	1.63 ± 0.15
SW-adapted	1.09 ± 0.06	99.3 ± 5.8	4.35 ± 0.17

Values represent the means ± SE of the aggregate weight, protein, and DNA of both glands from five animals. FW-adapted ducks ranged in age from 38–49 d. Those adapted to 1% NaCl were from 41–50 d old.

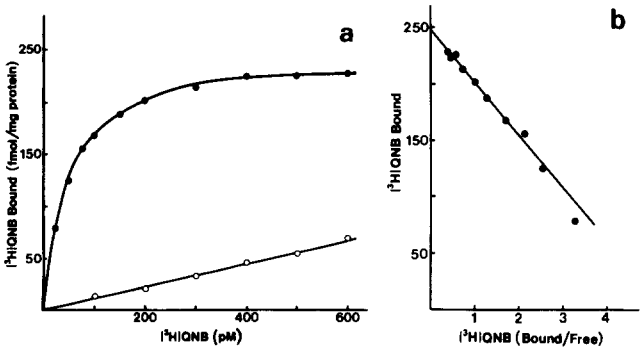

FIGURE 3 (*a*) Binding of [^{3}H]QNB to salt gland homogenate receptors from a FW-adapted duck expressed as a function of QNB concentration. Data is from a single experiment with all points determined in duplicate. Binding is related to particulate protein retained on the glass fiber filter. The incubation was carried out for 120 min at 37°C as described in Materials and Methods. Specific [^{3}H]QNB binding (●) was calculated from the difference in binding in the absence and presence (○) of 1 μM atropine sulfate. (*b*) Scatchard analysis of specific [^{3}H]QNB binding from the data shown in *a*. The calculated equilibrium dissociation constant (K_d) was 46.0 pM. Saturation binding (RL_{max}) was 248 fmol/mg particulate protein and the *r* was 0.984. Units on the ordinate are fmol/mg protein and on the abscissa are ml/mg protein.

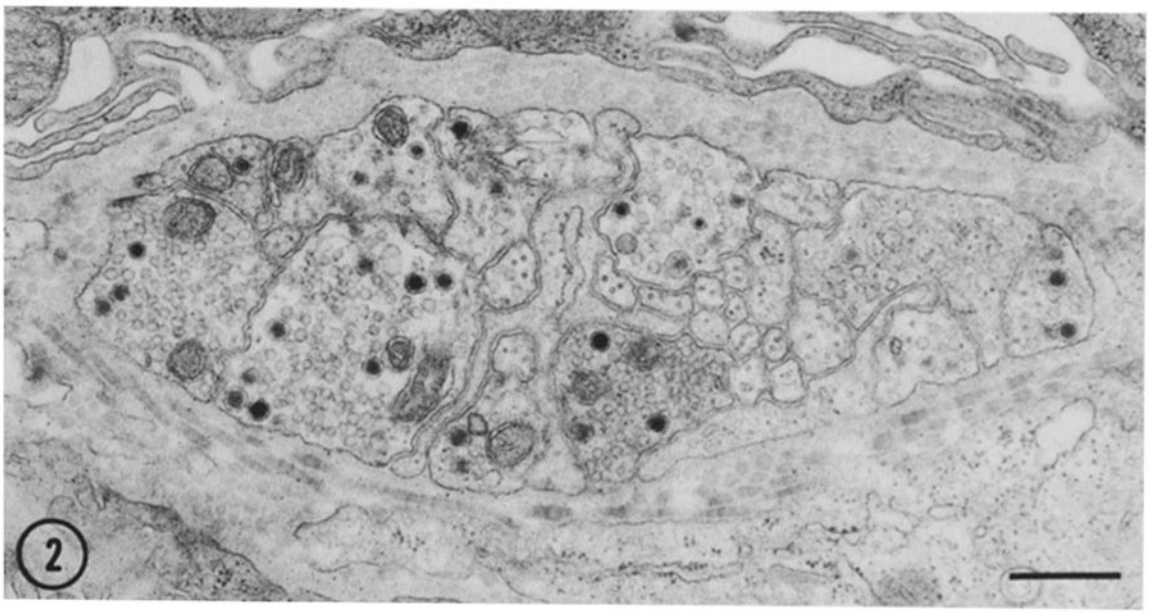

FIGURE 2 Electron micrograph of a nerve terminal in the salt gland of a FW-adapted duck. Basal plasma membrane folds of an adjacent secretory epithelial cell with associated mitochondria are visible at the top of the figure. The epithelial basal lamina and a thin band of collagen fibers separate nerve and epithelial cell membranes. Most nerve endings contain a homogenous population of small electron-lucent vesicles (30–40 nm) which presumably contain acetylcholine and a smaller number of larger dense-cored vesicles. Bar, 0.5 μm. × 28,900.

TABLE II

[^{3}H]QNB Binding to Salt Gland Homogenates from FW- and SW-adapted Ducks

		RL_{max}		
	K_d	Protein	DNA	pmol/ gland
	pM	*fmol/mg*	*fmol/μg*	
FW-adapted	40.1 ± 3.0	134 ± 9	1.73 ± 0.10	1.41 ± 0.09
		245 ± 17		
SW-adapted	35.1 ± 2.1	182 ± 11	4.16 ± 0.31	9.03 ± 0.86
		287 ± 20		

Values represent the means ± SE of determinations from homogenates of salt glands from five ducks adapted to each salinity regimen. RL_{max} in the second column is expressed as fmol of [^{3}H]QNB bound per milligram total protein (top) and particulate protein (bottom).

functional hypertrophy of the salt gland. The size of the receptor population does change, however. When binding of [^{3}H]QNB is related to protein retained on filters, a slight increase (from 245 to 287 fmol/mg protein) is noted in the salt-stressed glands. If, however, RL_{max} is expressed relative to the amount of protein present in the incubation, the calculated RL_{max} for both salinities is reduced and the differences between binding in FW and SW glands is increased to a significant extent. These changes result from the fact that a large percentage of total homogenate protein is soluble and is washed through the filters during rinsing. Comparison of protein present in the incubation medium with that collected on the filters showed that an average of 52.6% was retained from FW homogenates and 63.3% from homogenates of SW-adapted glands. The proportionately greater retention from SW homogenates is likely due to the fact that a larger percentage of cellular protein is membrane-associated in salt-stressed secretory cells. The average RL_{max} related to total glandular protein, both soluble and particulate, is 134 fmol/mg for FW homogenates and 182 fmol/mg for SW homogenates. The total amount of protein in a given salt gland increased ~4.7 times with saline adaptation (Table I). The total glandular muscarinic receptor population therefore increased by a factor of ~6.4. That a large percentage of this increase can be attributed to a greater number of muscarinic receptors per cell is shown when saturation binding is related to glandular DNA (Table II). FW-adapted salt glands bind 1.73 fmol [^{3}H]QNB/μg DNA while SW-adapted glands bind 4.16 fmol/μg, a highly significant difference ($P < 0.001$) of ~2.4-fold.

The saturation binding curves described above indicated that although [^{3}H]QNB binding sites were more numerous in SW-adapted glands, the dissociation constant for the receptor-antagonist complex in both FW-adapted and SW-adapted glands was identical. Determination of K_d by kinetic analysis was therefore attempted only on homogenates prepared from SW-adapted glands. The forward rate constant for the reaction (k_{+1}) was determined by incubating aliquots of homogenate in reaction buffer containing 100 pM [^{3}H]QNB for increasing time periods up to 120 min (Fig. 4). The association of [^{3}H]QNB with salt gland homogenate receptors reached equilibrium levels only after 90–120 min at this concentration of antagonist. Half-maximal binding was achieved by 14–15 min. Nonspecific binding in the presence of 1 μM atropine sulfate was not time-dependent and remained constant (~4% of specific binding) from the earliest time-point measured up to 120 min. Replotting the specific binding curve in semilogarithmic fashion (Fig. 4 *inset*) generated a single straight line ($r = 0.998$),

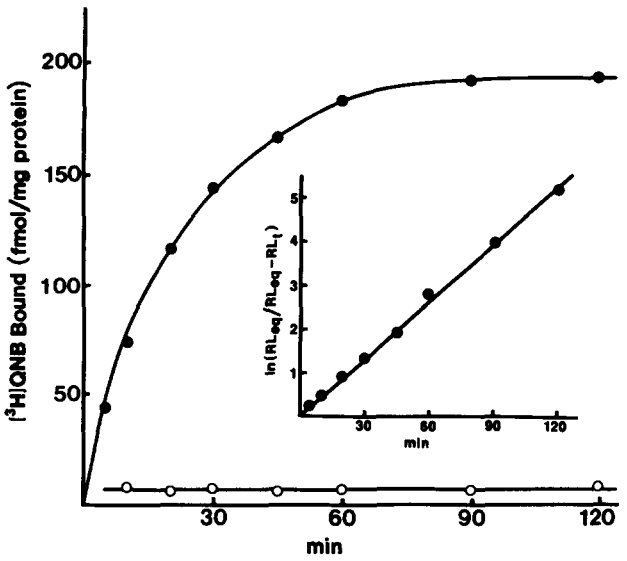

FIGURE 4 Binding of [^{3}H]QNB at 37°C to SW-adapted salt gland homogenate as a function of time (100 pM [^{3}H]QNB). Data points represent the average of three experiments, each carried out in duplicate. SE at each time-point were <10% of the respective mean values. Binding is expressed relative to particulate protein. Specific binding (●) was determined by subtraction of binding in the presence of 1 μM atropine sulfate (○) from binding in its absence (total binding). The *inset* shows specific binding data replotted in a semilogarithmic manner. *r*, 0.998. t_{50}, 15 min.

as would be expected if QNB binding under these conditions approximates a simple bimolecular reaction. The forward rate constant (k_{+1}) for the binding reaction, calculated as in Fields et al. (12), was $3.79 \times 10^8 \cdot M^{-1} \cdot min^{-1}$, similar to values obtained for rabbit iris (40), rat parotid gland (22), and rat brain (43).

The rate of dissociation of the antagonist-receptor complex was determined by incubating homogenates with 100 pM [^{3}H]QNB at 37°C for 120 min, adding 1 μM atropine sulfate, and sampling at intervals of up to 2 h thereafter. A semilogarithmic plot of [^{3}H]QNB bound relative to controls at 30-min intervals after atropine addition is shown in Fig. 5. The dissociation rate constant (k_{-1}) for this data, also calculated as in Fields et al. (12), was $7.78 \times 10^{-3} \cdot min^{-1}$ and the t_{50} for dissociation was 89 min. The ratio of k_{-1} to k_{+1} provided a calculated K_d of 20.5 pM, similar to that derived from equilibrium binding analysis.

Inhibition of [^{3}H]QNB Binding by Other Cholinergic Ligands

The pharmacological specificity of [^{3}H]QNB binding to SW homogenate receptors was investigated by analysis of the effects of other cholinergic antagonists, cholinergic agonists, and ion transport inhibitors on equilibrium binding. Competitive binding curves are shown in Fig. 6. From these data, Hill coefficients were determined (Fig. 7) along with the IC_{50} (concentration of inhibitor giving 50% reduction of [^{3}H]QNB binding) and apparent K_i ($K_i$app) for each competitive interaction. These values are presented in Table III.

Three muscarinic antagonists; atropine, scopolamine, and unlabeled QNB, all proved to be potent inhibitors of specific [^{3}H]QNB binding to homogenates of salt gland. Atropine and scopolamine were very similar in their competitive effects, with $K_i$app values of 587 and 546 pM, respectively. The Hill coef-

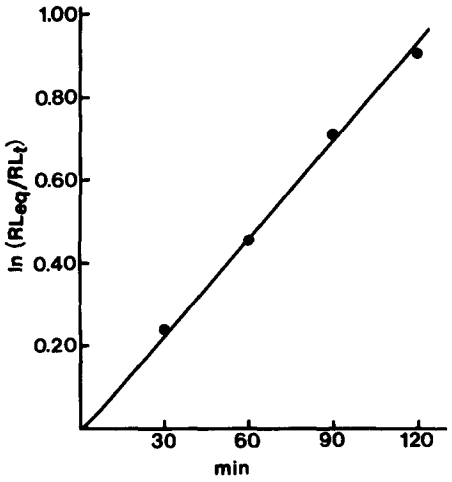

FIGURE 5 Rate of dissociation of [^{3}H]QNB bound as a function of time. Data points represent the average of three experiments on homogenates from SW-adapted animals, each carried out in duplicate. SE were <5% at each time-point. Homogenate was incubated for 120 min at 37°C with 100 pM [^{3}H]QNB. Atropine sulfate (1 μM) was added at $t = 0$ to one set of tubes. Specific binding in paired control and experimental tubes was determined at 30 min intervals after atropine addition. r, 0.996. t_{50}, 89 min.

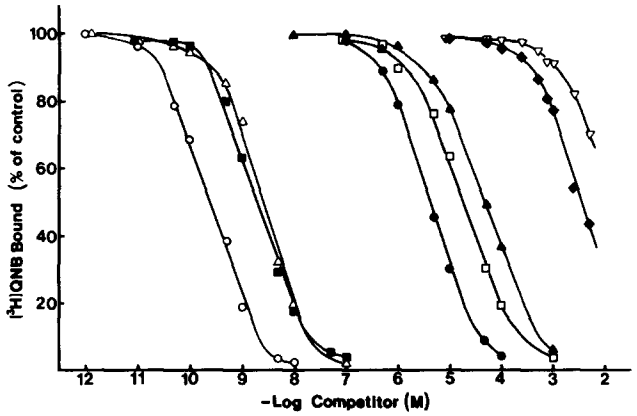

FIGURE 6 Inhibition of specific [^{3}H]QNB binding to SW-adapted salt gland homogenate by cholinergic agents and ion transport inhibitors. [^{3}H]QNB concentration was 100 pM. Incubations were carried out at 37°C for 120 min. Each curve represents the average of three experiments, except those for furosemide and bumetanide (four experiments each). ○, unlabeled DL-QNB; ■, scopolamine; △, atropine; ●, oxotremorine; □, methacholine; ▲, carbachol; ◆, furosemide; ▽, bumetanide

ficients for atropine and scopolamine were 0.997 and 0.927, in agreement with previous studies showing that Hill coefficients for antagonists are ~1 (12, 15, 20). Competition by unlabeled QNB gave a Hill coefficient of 1.008 and a $K_i$app of 61.6 pM. The IC_{50} for this inhibition was 237 pM, in good agreement with the expected value of 200 pM for inhibition of binding by this racemic mixture of active and inactive isomers.

Carbachol, methacholine, and oxotremorine also inhibited [^{3}H]QNB binding, although at much higher concentrations than did the antagonists tested. Oxotremorine was the most potent agonist, with a $K_i$app of 1.07 μM. The inhibition constants for methacholine and carbachol were 5.3 and 12.0 μM, respectively. Hill coefficients for methacholine and carbachol were somewhat lower than those detemined for antagonists,

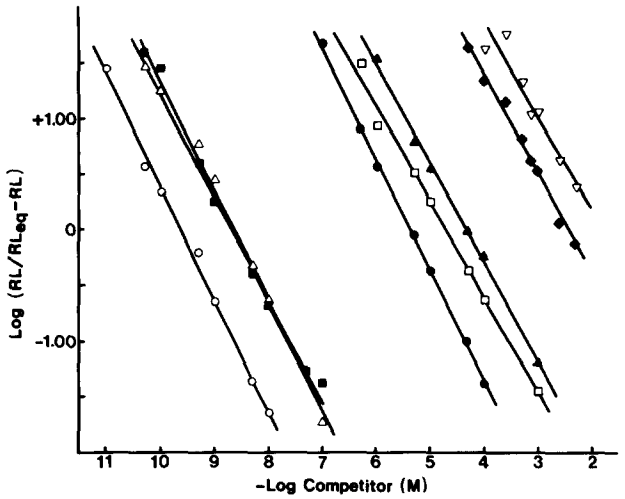

FIGURE 7 Hill plots of data from Fig. 6. The same symbols are used for individual ligands. RL_{eq} is equal to specific [^{3}H]QNB binding in the absence of competitors. RL represents the level of binding at various concentrations of competing drugs.

TABLE III

Effect of Drugs on [^{3}H]QNB Binding to Salt-Gland Homogenates

Drug	Hill coefficient	IC_{50}	$K_i$app
		μM	μM
Quinuclidinyl benzilate	1.008	0.000237	0.000062
Scopolamine	0.927	0.00210	0.000546
Atropine	0.997	0.00226	0.000587
Oxotremorine	0.995	4.11	1.068
Methacholine	0.858	20.4	5.30
Carbachol	0.889	46.2	12.00
Furosemide	0.901	3,600	935
Bumetanide	0.836	5,710	1,484

Hill coefficients were calculated as the negative slope of the regression lines for specific compounds in Fig. 7. IC_{50} values were also determined from Fig. 7. The inhibition constant ($K_i$app) for each compound was calculated using the equation: $K_i\text{app} = IC_{50}/1 + (L_T/K_d)$ derived from Fields et al. (12). $L_T = 100$ pM [^{3}H]QNB and K_d was taken as 35.1 pM.

although the coefficient for oxotremorine, 0.995, was not significantly different from 1.

The ion transport inhibitors ouabain and furosemide both interfere with certain transport related metabolic responses of salt gland cells to cholinergic stimulation (16, 17). Possible effects of both compounds on [^{3}H]QNB binding to the acetylcholine receptor were therefore examined. Ouabain at concentrations from 10 μM to 1 mM had no effect on binding. Furosemide, on the other hand, markely inhibited specific binding of [^{3}H]QNB to homogenate receptors (Figs. 6–9), as did the related loop diuretic bumetanide (Figs. 6 and 7). Inhibition constants for these two compounds were in the millimolar range (Table III), with furosemide being somewhat more potent. Examination of the effects of furosemide on [^{3}H]QNB binding as a function of time (Fig. 8), and on saturation binding of the labeled antagonist (Fig. 9), indicated that the observed inhibition was of the competitive type. Scatchard analysis of saturation binding isotherms (Fig. 9) performed in the presence of 1 or 5 mM furosemide invariably generated a single straight line that converged with the Scatchard line of the control curve at the same value for RL_{max}.

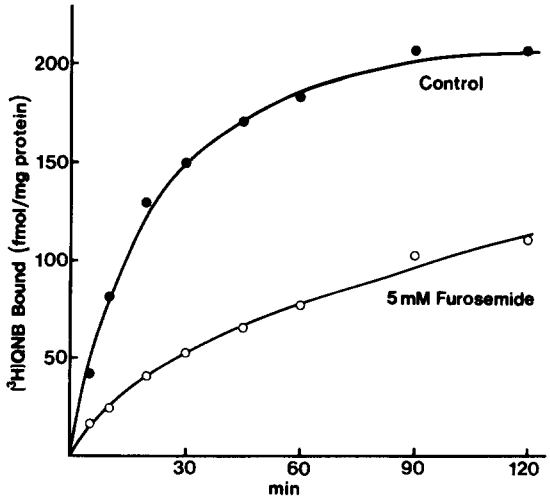

FIGURE 8 Effect of furosemide on specific [^{3}H]QNB binding to SW-adapted salt gland homogenate receptors as a function of time at 37°C. Results are from a single experiment, each point determined in duplicate, and related to particulate protein. [^{3}H]QNB concentration was 100 pM. ●, control. ○, 5 mM furosemide.

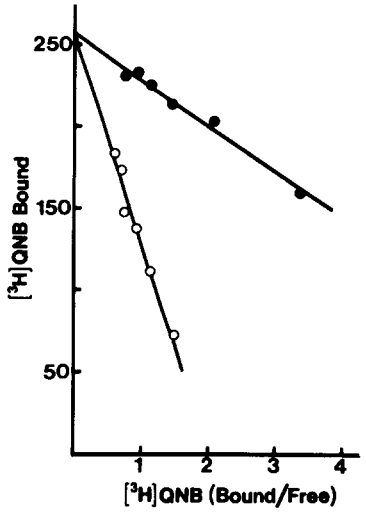

FIGURE 9 Scatchard analysis of specific [^{3}H]QNB saturation binding curves performed in the absence (●) and presence (○) of 5 mM furosemide at [^{3}H]QNB concentrations from 50 to 300 pM. Results are from a single experiment with all points done in duplicate. Incubations were carried out at 37°C for 120 min. RL_{max} for control binding in this experiment was 258 fmol/mg protein and the calculated K_d was 28.5 pM. In the presence of furosemide, RL_{max} was 256 fmol/mg protein and the K_d was 124.6 pM. Correlation coefficients for control and furosemide plots were 0.988 and 0.984, respectively.

To test whether an effect of furosemide on [^{3}H]QNB binding is also apparent in other tissues known to contain muscarinic acetylcholine receptors, we examined binding of the antagonist to homogenate receptors in rat atrium, brain, and exorbital lacrimal gland (Table IV). Homogenate from each tissue was incubated in the presence and absence of 5 mM furosemide for 120 min at 37°C. Under these conditions, the diuretic depresses [^{3}H]QNB binding to salt gland homogenate by 40–60%. No decrease in binding was seen, however, when homogenate from either brain or atrium was incubated, although a decrease of ~20% was noted for binding of the labeled antagonist to homogenates of lacrimal gland.

TABLE IV

Effect of Furosemide on [^{3}H]QNB Binding

Tissue	*n*	Specific [^{3}H]QNB bound: Control	Specific [^{3}H]QNB bound: 5 mM Furosemide	*P*
		pmol/g tissue		
Duck salt gland (SW)	5	13.3 ± 1.4	5.2 ± 0.6	0.001
Rat atrium	4	35.4 ± 2.3	36.6 ± 2.1	0.500
Rat brain	4	80.8 ± 2.1	79.4 ± 1.8	0.500
Rat lacrimal gland	4	12.9 ± 0.3	10.4 ± 0.3	0.005

Specific [^{3}H]QNB bound is expressed as the mean ± SE of duplicate determinations from *n* separate animals. Homogenate from respective organs was incubated with 100 pM [^{3}H]QNB for 120 min at 37°C.

DISCUSSION

This report describes and quantitates muscarinic acetylcholine receptors in the salt glands of domestic ducks adapted to conditions of low (FW) and high (SW) salt stress. Characterization of these receptors using the radiolabeled antagonist, [^{3}H]QNB, shows them to be similar to muscarinic receptors from various mammalian sources, including rabbit iris (40), rat brain (43), rabbit heart (12), rat parotid gland (22), and rat parietal cells (7). Muscarinic receptors exhibiting similar pharmacological specificities and affinity for [^{3}H]QNB have also recently been demonstrated in amphibian heart (15) and in cultured neural cell lines (5, 20, 38).

In the duck salt gland, cholinergic muscarinic receptors can be defined as a single class of saturable, high-affinity binding sites with respect to their interaction with [^{3}H]QNB. Saturation binding isotherms for both FW- and SW-adapted glands, when analyzed by the method of Scatchard (34), produced single straight lines with r typically between 0.95 and 1.00. The low dissociation constants derived from these analyses, 40.1 pM for FW-adapted and 35.1 pM for SW-adapted glands, demonstrate the very high affinity of the receptor in the duck salt gland for the labeled antagonist. Comparably determined K_d values for the receptor in several mammalian tissues and in amphibian heart have ranged from 10 to 70 pM, although much higher values such as the K_d of 0.78 nM for rat parietal cells (7) have occasionally been reported. As pointed out by Fields et al. (12), such a discrepancy may result from the dependence of K_d on receptor concentration in the assay. At concentrations of receptor >20 pM, values for K_d significantly above the true value can be expected (see Fig. 3 in Fields et al. [12] and Fig. 2 in Ludford and Talamo [22]). This problem was largely avoided in this study by adjusting the receptor concentrations in assays to levels of 12 pM or less. K_d values determined at three concentrations of receptor below this level showed a slight but nonsignificant dependence on receptor concentration in the assay. The average K_d values listed in Table II may therefore be slightly, but not significantly, higher than the true receptor equilibrium dissociation constants. Aside from supporting the phylogenetic constancy of receptor affinity for QNB, results of these saturation binding studies demonstrated that the affinity of the salt gland muscarinic receptor for [^{3}H]QNB remains the same regardless of the frequency of salt-stress induced receptor activation. Experimentally induced changes in the frequency of receptor activation in cultures of embryonic chick brain cells (38) and in rat parotid gland (41) likewise have failed to elicit major shifts in receptor-antagonist affinity.

Determination of the dissociation constant for the muscarinic receptor in SW-adapted glands from kinetic analysis of binding (Figs. 4 and 5) gave a value of 20.5 pM, similar to that previously calculated from saturation binding isotherms. In addition, these studies demonstrated that the kinetics of both formation and dissociation of the receptor-QNB complex are consistent with a simple bimolecular reaction mechanism under the standard conditions of incubation (37°C, 100 pM [^{3}H]-QNB). Other, more extensive, kinetic studies of ligand-muscarinic receptor interactions (15, 18, 19, 36), however, have presented convincing evidence that the actual reaction mechanism is more complex. Available data now support the view that binding occurs in two steps; a fast binding step leading to a relatively low affinity receptor-antagonist complex, followed by a slower isomerization reaction that probably involves a conformational change in the receptor molecule. This second reaction step markedly increases the stability of the complex. Formation and dissociation of the low affinity complex is too rapid at 37°C to be characterized by the filtration method used in this study, and it is thus the isomerization reaction that is characterized by the rate constants derived from data in Figs. 4 and 5. Nonetheless, the kinetic data clearly support the results from saturation binding studies and demonstrate the presence in the duck salt gland of receptors with high affinity for [^{3}H]-QNB.

While the affinity of the muscarinic acetylcholine receptor for QNB appears to be the same in the salt glands of ducks adapted both to FW and to water with 1% NaCl, the receptor population is clearly increased in the latter (Table II). Since the DNA content of individual cells in the salt gland remains the same regardless of conditions of salt stress (16), relating [^{3}H]QNB binding to DNA allows calculation of average numbers of receptors per cell. On making this calculation, it becomes apparent that individual salt gland cells contain approximately three times as many muscarinic receptors in SW glands as do their nonstressed counterparts. The calculated numbers of receptors per cell, 5,800 in FW-adapted and 14,100 in SW-adapted glands, are in the range previously reported by Ecknauer et al. (7) for parietal cells (4,900) and by Putney and Van De Walle (31) for parotid acinar cells (23,000). Our results thus provide direct evidence for *de novo* synthesis of muscarinic cholinergic receptors during the plasma membrane hypertrophy that typifies the response of salt gland epithelial cells to chronic salt stress. It is tempting to speculate that this upward regulation of receptors may represent a mechanism by which the sensitivity of the secretory cell to cholinergic stimulation is increased concurrent to the potentiation of cellular transport efficiency provided by increases in basolateral plasma membrane, mitochondria, and Na^+,K^+-ATPase (8, 9, 10).

Binding of [^{3}H]QNB to salt gland muscarinic acetylcholine receptors is inhibited, as expected, by other cholinergic antagonists and by agonists as well (Fig. 6). The efficacy of blockade by antagonists is several orders of magnitude greater than is that of the latter group of compounds, as has been observed previously for ligand-muscarinic receptor interactions in other tissues (7, 12, 15). A surprising finding in this study was the observed inhibition of [^{3}H]QNB binding by the diuretics furosemide and bumetanide (Fig. 6). Furosemide and bumetanide interfere with electrogenic ion transport across both secretory and absorptive epithelia, presumably by inhibiting a putative facilitated transport carrier that couples the uptake of Na^+ and Cl^- across the plasma membrane of epithelial cells as an electrically silent ion pair (13). In some epithelia, bumetanide appears to be a more potent inhibitor of ion transport processes, although this may not be the case in the duck salt gland. We have recently shown that exposure of dispersed salt gland cells to 1 mM furosemide abolishes the increase in cellular oxygen consumption elicited by cholinomimetics (17). In preliminary experiments, bumetanide at this concentration blocked only 60% of this increase. Thus in the duck salt gland, the relative potency of the two diuretics in inhibiting cholinergic stimulation of at least one metabolic parameter coincides with their effectiveness in displacing [^{3}H]QNB binding.

In view of the relatively high concentrations of furosemide and bumetanide required to displace [^{3}H]QNB binding to muscarinic receptors in the salt gland ($K_i$app $\cong$ 1 mM) and the comparatively lower concentrations (IC_{50} = 10^{-6} to 10^{-4} M) which effectively inhibit ion transport processes in epithelia, the effect of the diuretics on [^{3}H]QNB binding might be interpreted as due to a nonspecific effect on membrane or receptor structure. However, considering the apparent specificity of furosemide and related diuretics on ion transport processes in the avian salt gland (17) and in other transporting epithelia (21, 33), the interaction with the muscarinic receptor may be more than fortuitous. As shown in Figs. 8 and 9, the interaction of furosemide with [^{3}H]QNB is of a directly competitive nature. The proportional reduction of binding caused by furosemide is greatest at early time points (Fig. 8) and steadily decreases relative to controls at longer intervals, presumably because of the much greater affinity of the receptor for [^{3}H]QNB. Intersection of Scatchard plot lines drawn from saturation binding isotherms carried out in the absence and presence of furosemide (Fig. 9) at identical values for RL_{max} likewise suggests a competitive interaction (3). A strictly competitive response would not be expected if the diuretic exerted its effects on [^{3}H]QNB binding via a general deleterious interaction with, for instance, membrane protein. The absence of an effect of furosemide on [^{3}H]QNB binding in rat atrium and brain (Table IV) also argues against such a nonspecific process. The data are consistent, therefore, with the possibility that furosemide binds, albeit with low affinity, to a site on the muscarinic receptor or to a closely associated interactive site on the salt gland plasma membrane. While additional data are clearly required to further substantiate this hypothesis, functional correlations for such an association are intriguing. Recent studies with salt glands (17) indicate that furosemide blocks increases in oxygen consumption and Na^+ pump activity elicited by methacholine, as does removal of either Na^+ or Cl^- from the medium bathing the cells. The diuretic has only minor effects on these two parameters in unstimulated cells. These data indicate that activation of a furosemide-sensitive mechanism for the uptake of Na^+ and Cl^- is an initial step in stimulus-response coupling in the salt gland cell. In addition, activation of muscarinic receptors in other secretory epithelia, including those of mammalian lacrimal (23, 24, 29) and parotid glands (28) and exocrine pancreas (30, 32), also stimulates cellular Na^+ and Cl^- uptake. The available evidence thus suggests that muscarinic acetylcholine receptors in at least some exocrine glands control the functional status of ion channels in the plasma membrane that mediate the uptake of Na^+ and Cl^-. Whether these channels are sensitive to blockade by furosemide in all these epithelia remains to be elucidated. Our data indicate that at least in the duck salt gland and rat lacrimal gland the receptors for furosemide and [^{3}H]QNB may exhibit a close spacial as well as metabolic association. The lack of a furosemide effect on [^{3}H]QNB binding to muscarinic acetylcholine

receptors in rat atrium and brain (Table IV) demonstrate a functional heterogeny in receptors or their immediate membrane environments in separate tissues within the same animal. Differences in agonist discrimination between rat ileal and ganglionic muscarinic receptors also have been reported recently (4), providing support for this possibility.

The results discussed demonstrate the presence of a population of muscarinic acetylcholine receptors in the avian salt gland cell, the numbers of which are modulated by functional demand, i.e., by chronic salt stress, on the gland. These receptors also may be associated with a furosemide-sensitive ion channel, although proof for such an association must await the development of suitable ligands for the *in situ* localization at high resolution of these two membrane elements and their isolation and molecular characterization.

The authors thank Mr. James H. Schreiber and Ms. Lynn K. Richardson for their excellent technical assistance and Drs. Gary L. Peterson and Michael I. Schimerlik for their comments during preparation of this manuscript.

This research was supported by U.S. Public Health Service grant AM 27559.

Received for publication 6 April 1981, and in revised form 10 August 1981.

REFERENCES

1. Ash, R. W., J. W. Pearce, and A. Silver. 1969. An investigation of the nerve supply to the salt gland of the duck. *Q. J. Exp. Physiol. Cogn. Med. Sci.* 54:281–295.
2. Borut, A., and K. Schmidt-Nielsen. 1963. Respiration of avian salt-secreting gland in tissue slice experiments. *Am. J. Physiol.* 204:573–581.
3. Barestrup, C., and M. Nielsen. 1980. Multiple benzodiazepine receptors. *Trends in Neuroscience.* 3:301–303.
4. Brown, D. A., A. Forward, and S. March. 1980. Antagonist discrimination between ganglionic and ileal muscarinic receptors. *Brit. J. Pharmacol.* 71:362–364.
5. Burgermeister, W., W. L. Klein, M. Nirenberg, and B. Witkop. 1978. Comparative binding studies with cholinergic ligands and histrionicotoxin at muscarinic receptors of neural cell lines. Mol. Pharmacol. 14:751–767.
6. Croft, D. N., and M. Lubran. 1965. The estimation of deoxyribonucleic acid in the presence of sialic acid: application to analysis of human gastric washings. *Biochem. J.* 95: 612–620.
7. Ecknauer, R., W. J. Thompson, L. R. Johnson, and G. C. Rosenfield. 1980. Isolated parietal cells: [^{3}H]QNB binding to putative cholinergic receptors. *Am. J. Physiol.* 239: G204–G209.
8. Ernst, S. A., and R. A. Ellis. 1969. The development of surface specialization in the secretory epithelium of the avian salt gland in response to osmotic stress. *J. Cell Biol.* 40: 305–321.
9. Ernst, S. A., and J. W. Mills. 1977. Basolateral plasma membrane localization of ouabain-sensitive sodium transport sites in the secretory epithelium of the avian salt gland. *J. Cell Biol.* 75:74–94.
10. Ernst, S. A., C. C. Goertemiller, Jr., and R. A. Ellis. 1967. The effect of salt regimens on the development of (Na^+-K^+)-dependent ATPase activity during the growth of salt glands of ducklings. *Biochim. Biophys. Acta.* 135:682–692.
11. Fänge, R., K. Schmidt-Nielsen, and M. Robinson. 1958. Control of secretion from the avian salt gland. *Am. J. Physiol.* 915:321–326.
12. Fields, J. Z., W. R. Roeske, E. Morkin, and H. I. Yamamura. 1978. Cardiac muscarinic cholinergic receptors: biochemical identification and characterization. *J. Biol. Chem.* 253: 3251–3258.
13. Frizzell, R. A., M. Field, and S. G. Schultz. 1979. Sodium-coupled chloride transport by epithelial tissues. *Am. J. Physiol.* 236:F1-F8.
14. Hanwell, A., and M. Peaker. 1975. The control of adaptive hypertrophy in the salt glands of geese and ducks. *J. Physiol (Lond.).* 248:193–205.
15. Hartzell, H. C. 1980. Distribution of muscarinic acetylcholine receptors and presynaptic nerve terminals in amphibian heart. *J. Cell Biol.* 86:6–20.
16. Hootman, S. R., and S. A. Ernst. 1980. Dissociation of avian salt gland: separation procedures and characterization of dissociated cells. *Am. J. Physiol.* 238:C184–C195.
17. Hootman, S. R., and S. A. Ernst. 1981. Effect of methacholine on Na^+ pump activity and ion content of dispersed avian salt gland cells. *Am. J. Physiol.* 241:R77–R86.
18. Järv, J., B. Hedlund, and T. Bartfai. 1979. Isomerization of the muscarinic receptor-antagonist complex. *J. Biol. Chem.* 54:5595–5598.
19. Järv, J., B. Hedlund, and T. Bartfai. 1980. Kinetic studies on muscarinic antagonist-agonist competition. *J. Biol. Chem.* 225:2649–2651.
20. Klein, W. L. 1980. Multiple binding states of muscarinic acetylcholine receptors in membranes from neuroblastoma X glioma hybrid cells. *Biochem. Biophys. Res. Commun.* 93:1058–1066.
21. Ludens, J. H., W. B. Zimmerman, and J. R. Schnieders. 1980. Nature of the inhibition of Cl^- transport by furosemide: evidence for a direct effect on active transport in toad cornea. *Life Sci.* 27:2453–2458.
22. Ludford, J. M., and B. R. Talamo. 1980. β-Adrenergic and muscarinic receptors in developing rat parotid glands. *J. Biol. Chem.* 255:4619–4627.
23. Parod, R. J., and J. W. Putney, Jr. 1980. Stimulus-permeability coupling in rat lacrimal gland. *Am. J. Physiol.* 239:G106–113.
24. Parod, R. J., B. A. Leslie, and J. W. Putney, Jr. 1980. Muscarinic and α-adrenergic stimulation of Na and Ca uptake by dispersed lacrimal cells. *Am. J. Physiol.* 239:G99–G105.
25. Peaker, M., and J. L. Linzell. 1975. Salt Glands in Birds and Reptiles. Cambridge University Press, Cambridge.
26. Peterson, G. L. 1977. A simplification of the protein assay method of Lowry et al. which is more generally applicable. *Anal. Biochem.* 83:346–356.
27. Pittard, J. B., and A. D. Hilly. 1973. The effect of denervation on genotypic and compensatory growth of the immature avian salt gland. *J. Anat.* 114:303.
28. Putney, J. W., Jr. and R. J. Parod. 1978. Calcium-mediated effects of carbachol on cation pumping and Na uptake in rat parotid gland slices. *J. Pharmacol. Exp. Ther.* 205:449–458.
29. Putney, J. W., Jr., and C. M. Van De Walle. 1979. Effect of carbachol on ouabain-sensitive uptake of ^{86}Rb by dispersed lacrimal gland cells. *Life Sci.* 24:1119–1124.
30. Putney, J. W., Jr., and C. M. Van De Walle. 1980. Role of calcium in stimulation of ^{36}Cl uptake by dispersed pancreatic acinar cells. *Biochem. Biophys. Res. Commun.* 95:1461–1466.
31. Putney, J. W., Jr., and C. M. Van De Walle. 1980. The relationship between muscarinic receptor binding and ion movements in rat parotid cells. *J. Physiol (Lond.).* 299:521–531.
32. Putney, J. W., Jr., C. A. Landis, and C. M. Van De Walle. 1980. Effect of carbachol on radiosodium uptake by dispersed pancreatic acinar cells. *Pflügers Arch.* 385:131–136.
33. Saito, Y., K. Itoi, K. Horiuchi, and T. Watanabe. 1980. Mode of action of furosemide on the chloride-dependent short-circuit current across the ciliary body epithelium of toad eyes. *J. Membr. Biol.* 53:85–93.
34. Scatchard, G. 1949. The attractions of proteins for small molecules and ions. *Ann. N. Y. Acad. Sci.* 51:660–672.
35. Schiller, G. D. 1979. Reduced binding of (^{3}H)-quinuclidinyl benzilate associated with chronically low acetylcholinesterase activity. *Life Sci.* 24:1159–1164.
36. Schimerlik, M. I., and R. P. Searles. 1980. Ligand interactions with membrane-bound porcine atrial muscarinic receptors(s). *Biochemistry.* 19:3407–3413.
37. Shifrin, G. S., and W. L. Klein. 1980. Regulation of muscarinic acetylcholine receptor concentration in cloned neuroblastoma cells. *J. Neurochem.* 34:993–999.
38. Siman, R. G., and W. L. Klein. 1979. Cholinergic activity regulates muscarinic receptors in central nervous system cultures. *Proc. Natl. Acad. Sci. U. S. A.* 76:4141–4145.
39. Stewart, D. J., J. Sax, R. Funk, and A. K. Sen. 1979. Possible role of cyclic GMP in stimulus-secretion coupling by salt gland of the duck. *Am. J. Physiol.* 237:C200–C204.
40. Taft, W. C., Jr., A. A. Abdel-Latif, and R. A. Akhtar. 1980. [^{3}H]WB-4101 binding to alpha-adrenergic receptors in rabbit iris. *Biochem. Pharmacol.* 29:2713–2720.
41. Talamo, B. R., S. C. Adler, and D. R. Burt. 1979. Parasympathetic denervation decreases muscarinic receptor binding in rat parotid. *Life Sci.* 24:1573–1580.
42. Van Rossum, G. D. V. 1966. Movements of Na^+ and K^+ in slices of herring gull salt gland. *Biochim. Biophys. Acta.* 126:338–349.
43. Yamamura, H. I., and S. H. Snyder. 1974. Muscarinic cholinergic binding in rat brain. *Proc. Natl. Acad. Sci. U.S.A.* 71:1725–1729.